Dynamic Behavior of Unbonded Partially Post-Tensioned Concrete Beams under Cyclic Loading.

H. El-Esnawi[1] and A. Hafiz[2]

[1]Ass. Prof. Civil Engineering Dept., Faculty of Engineering, Al-Azhar University, Cairo, Egypt
[2]Lecturer Civil Engineering Dept., Faculty of Engineering, Al-Azhar University, Cairo, Egypt
hesnawi2000@yahoo.com

Abstract: Three unbonded partial post-tensioned concrete beams with variable PPR in addition to one unbonded fully post-tensioned beam are tested under cyclic vertical displacement to investigate the dynamic behaviors of partially and fully post-tensioned concrete beams. The failure patterns, skeleton curves, hysteretic model, displacement restoring capacity, ductility, stiffness degradation and energy dissipation capacity of all beams are discussed. Studies indicate that the partially post-tensioned beams behave in a more ductile manner in comparison with a fully post-tensioned beam. Relatively high deformation restoring capacity could also be observed clearly in the fully post-tensioned beam. Tests also show that the energy dissipation capacity of partially post-tensioned beams is significantly higher than fully post-tensioned beams. Stiffness degradation of partially post-tensioned beams was higher than the fully post-tensioned.
[H. El-Esnawi and A. Hafiz. **Dynamic Behavior of Unbonded Partially Post-Tensioned Concrete Beams under Cyclic Loading..** *Life Sci J* 2018;15(3):18-27]. ISSN: 1097-8135 (Print) / ISSN: 2372-613X (Online). http://www.lifesciencesite.com. 3. doi:10.7537/marslsj150318.03.

Keywords: post-tensioned, cyclic loading, PPR Ratio, Stiffness degradation, displacement restoring capacity, energy dissipation capacity

1. Introduction:

Pre-stressing is a technique that has been widely used for decades in all sorts of concrete structures. Its ability to minimize reinforcement congestion, decrease deflection, and control cracking under service loads has made it a widely popular choice for large spans and for the precast industry.

The current edition of the ACI Building Code (ACI 318–2014) [1] now recognizes Four classes of pre-stressed flexural members, A, B, C, and D. Under full service load. The dividing lines between the four classes are based on nominal tensile stresses in the pre-compressed tensile zone. The ACI Building Code (ACI 318–2014) [1] limited the design of these members to the full pre-stressed case. Which have allowable tensile stress equal zero. Partially pre-stressed concrete offers several advantages over fully pre-stressed. *The overall objective* of this study was to determine the viability of unbonded partially post-tensioned concrete members under the impact of cyclic loading.

The difference between fully and partially pre-stressed concrete beams is referred to the allow- able permissible tension stresses [1]. Fully pre-stressing is de- fined as a complete elimination of tensile stresses in members at full service load or allow small tension stresses, which can be resisted by concrete only, while partially pre-stressing allow for higher tension stresses in concrete and cracking under full service loads [2,3]. In this research, the partially pre-stressed concrete beams were achieved with a combination of pre-stressed and non-pre-stressed reinforcement while fully pre- stressed concrete beams contained pre-stressed reinforcement only.

Manalip et al. [3], studied the behavior of the compression zone of reinforced and pre-stressed HSC elements and concluded that HSC has a brittle behavior in case of specimens subjected to axial compression, while different behavior was observed for reinforced or pre-stressed beams. It was also re-ported that use of HSC results in doubling the plastic rotation capacity, for reinforced or pre-stressed concrete beams subjected to pure flexural stresses.

Xiao and Ma [4] investigated the seismic performance of HSC beams in moment resisting frame structures. Two large scale HSC and two counterpart normal-strength concrete model beams were tested under cyclic shear and double bending. Studies showed that both high-strength and normal-strength concrete beams developed ductile flexural responses. The HSC beams exhibited increased capacity and improved hysteretic performance compared to normal-strength concrete beams.

2. Experimental Program:

2.1. Description of specimens

A total of four half scale unbonded post-tensioned simple beams were tested under cyclic load up to failure. The main parameter among the tested specimens is the pre-compression value which can also be definite as the partially pre-stressed ratio (PPR).

Figs. (1), show the specimen's dimensions, internal reinforcement, cable profile, and support

arrangement for all tested specimens. All tested specimens had a typical R-shaped cross-section and equal spans. All beams had the same dimensions with a total length of 4700 mm, clear span of 4500 mm, beam width of 150 mm, and an overall height of 350 mm, as shown in the figures. All beams were designed to have the same ultimate moment capacity. Cable profiles are the same for all beams. In order to prevent the occurrence of shear failure prior to the flexural failure, the shear reinforcement of all specimens were consisting of two 10 mm vertical branches with horizontally spaced 100 mm at the maximum shear zone, and 150mm spacing at zero shear zone. In addition, the transverse reinforcement of the compression zone consisted of 10 mm diameter bars, and variable tensile reinforcement. All the pre-stressing cables comprised of seven wires with a nominal diameter 0.6 in which equal to 15.24 mm for partially and fully post-tensioned beams. The main parameter among the tested specimens is the partial pre-stressing ratio (PPR). The four tested specimens were coded as following B1-25-FP-1, B2-25-PP-0.87, B3-25-PP-0.73 and B4-25-PP-0.62, and only one cable in order to simulate the post tensioning system. Specimen's details, mechanical properties for reinforcing bars, and mechanical properties of used materials are listed in Table (1) & (2).

Table (1). Details of tested specimens

Details of specimens	Beam specimens			
	B1-25-FP-1	B2-25-PP-0.87	B3-25-PP-0.73	B4-25-PP-0.62
Top RFT	2Φ10	2Φ10	2Φ10	2Φ10
Bottom RFT	-------	2Φ8	2Φ10	2Φ12
Shear RFT	10Φ10/m	10Φ10/m	10Φ10/m	10Φ10/m
PT strand	0.6"	0.6"	0.6"	0.6"
PPR ratio	1	0.87	0.73	0.62

* Where (B1, B2, B3----) are the beams codes which are given as the beam number.
* The value (25) refers to concrete compressive strength.
* FP or PP refers to fully or partially post-tensioned respectively.
* The value (1, 0.87, 0.73, and 0.62) refers to (PPR).

Table (2). Mechanical properties of concrete

Mechanical properties	Beam specimens			
	B1-25-FP-1	B2-25-PP-0.87	B3-25-PP-0.73	B4-25-PP-0.62
F'_c (mPa)	31.17	31.17	31.17	31.17
F_t (mPa)	2.9	2.9	2.9	2.9

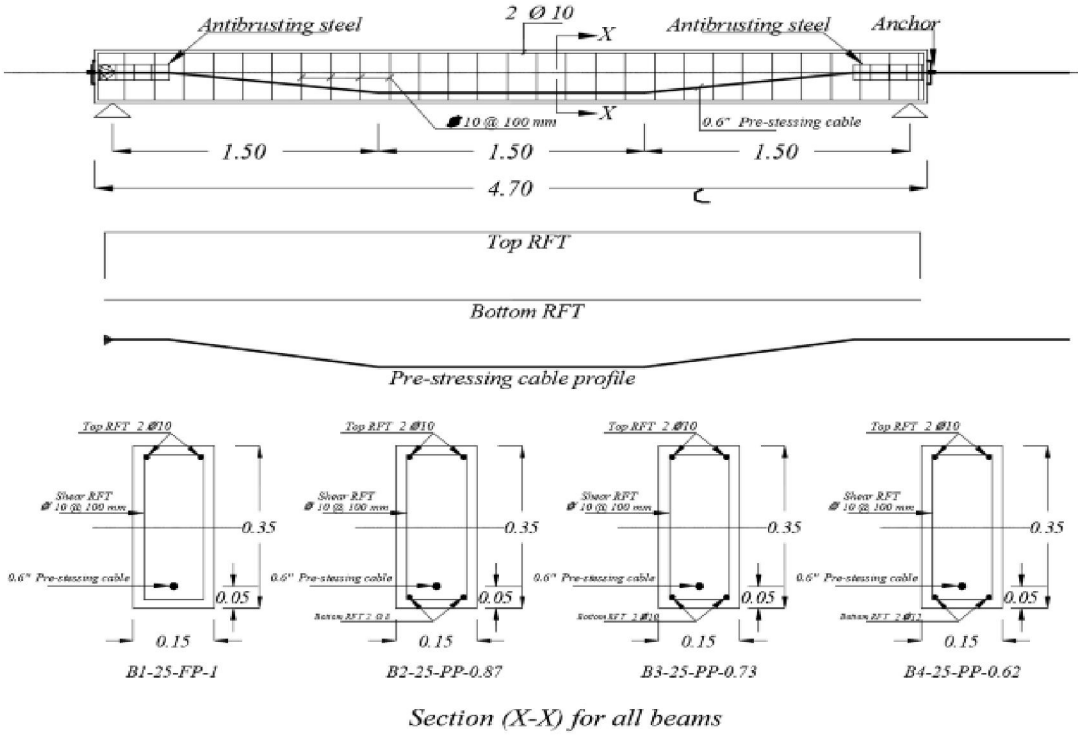

Fig. (1) Reinforcement details ofspecimen's

2.2. Specimen's fabrication and pre-stressing process.

Plywood forms were prepared for casting the concrete in the laboratory of AL-AZHAR University. All forms had the same dimensions. The steel reinforcement cages were prepared and put into the forms. Corrugated plastic ducts for strands were accurately and symmetrically installed about mid-span in the forms. Two end-bearing plates were positioned at the two ends of all beams to distribute the pre-stressing force over all the cross sections of the beams in order to avoid any cracks in the anchorage zone.

The concrete was compacted for two minutes after casting, using an electrical poker vibrator, followed by water curing and covering with polythene sheeting for one week. For control purposes, 6 cylinders with 150 mm diameter and 300 mm height, were cast alongside the specimens from the same concrete batch and were cured with the specimens. The cylinders were tested before pre-stressing and at the same day of testing the beams. Table (2) shows the average cylinder strength after two months from casting of the concrete. Fig (2) shows the forms, reinforcement cages and curing process.

The pre-stressing force was applied at 75% of the ultimate strength of the strands. One mono barrel anchor was installed at one end of the beams since all beams had one live end and deed end. A calibrated hydraulic jack was used in the pre-stressing process. The stressing forces were transferred from the hydraulic jack to the strands along four equal stages ranging from 25% to 100% of the required force. The force in the strands was measured through the elongation of the strands which was measured at every stressing stage. Pre-stressing presses was done immediately before testing to avoid occurrence of long term losses. Fig (3) shows the pre-stressing process.

2.3. Instrumentation

Two Linear Variable Distance Transducers (LVDTs) with 0.01 mm accuracy were used to measure the mid-span deflections of all beams, as shown in Fig. (4). The electrical resistance strain gauges, which were attached to steel bars and concrete, were connected to a data acquisition system to record the data. Finally, the data were collected using a data acquisition system and ‘‘lab view’’ software at a rate of 2 sample per seconds.

2.4. Test setup and loading procedure.

Fig. (4) Shows the details of the test set-up. It should be noted that the test arrangement was symmetrical about the mid-span section of all beams. Each beam was loaded in two loading points bending. The beams were subjected to a uni-directional cyclic loading up to failure, using a hydraulic actuator of 250 kN capacity. The load was applied on the beams using a stroke displacement control system, which divided the machine load that was applied through a steel spreader beam 1.5 m in length, as shown in the figure. The cyclic loading was achieved by increasing the stroke with 2 mm increments each two cycles untilfailure. As shown in fig (5).

Fig (2) Forms, reinforcement cages and curing process.

Fig (3) Pre-stressing process.

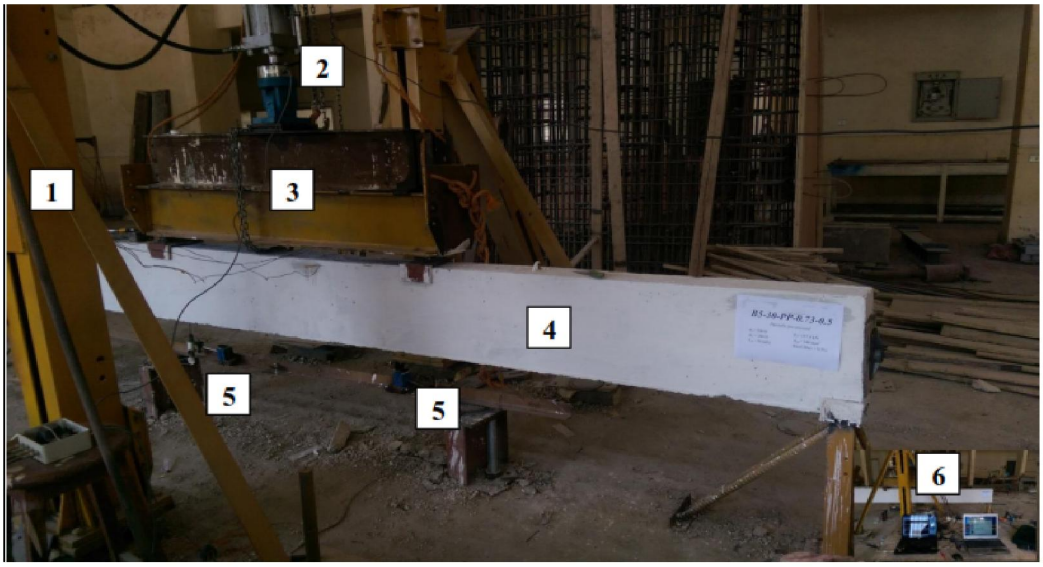

1) Loading frame
2) Hydraulic actuator.
3) Steel spreader beam
4) Tested specimen
5) LVDT
6) Data acquisition system

Fig (4) Test set up.

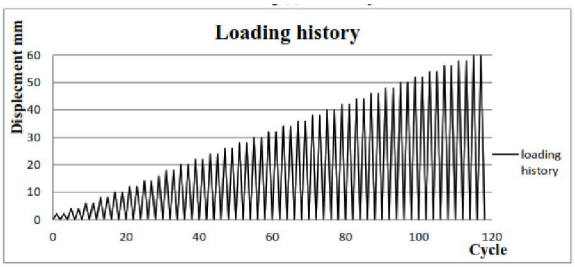

Fig (5) Loading history

3. Test results and discussion.

3.1 Crack pattern and failure mode.

Fig. (6) Shows the crack patterns at failure of all tested beams and Table (3) Summarize the details of the test process of all beams. On the other hand, Fig. (7) Shows the total load versus the mid span deflection of all tested beams.

1. Flexural cracks initiated at pure bending sections of beams. During the +14Δy loading process, flexure-shear cracks could not be observed. Flexural cracks penetrating over the full depth of beam sections. After that, the existing cracks kept on

increasing with occurrence of new cracks. Finally, more vertical cracks and a few inclined cracks could be observed around the mid-span sections of beams.

2. When the width of cracks was less than 0.3 mm, cracks at the bottom of post-tensioned beams were almost closed, accompanied by very small residual deformation during the unloading, which indicated that the pre-stressed members behaved with large capacities in crack and deformation restoring.

3. For fully post-tensioned beams, the crack propagation followed similar traditional flexural patterns in simple beams and the first tension cracks appeared in the constant moment zone. In addition, less number of cracks with large crack width could observe at failure. Beam with PPR= 1 (fully pre-stressed) failed in compression due to crushing of concrete in the compression zone buckling of top steel bars. On the other hand, in partially post-tensioned beams large number of cracks with small crack width was observed. In fact, Conventional ductile flexural failure occured due to cutting of the main bottom steel followed by concrete crushing.

4. Failure patterns for all specimens were dominated by flexural effects. It could be observed that concrete crushed and spalled off at pure bending zone with a buckling of longitudinal steel bars. All failures occurred under extremely large deformations.

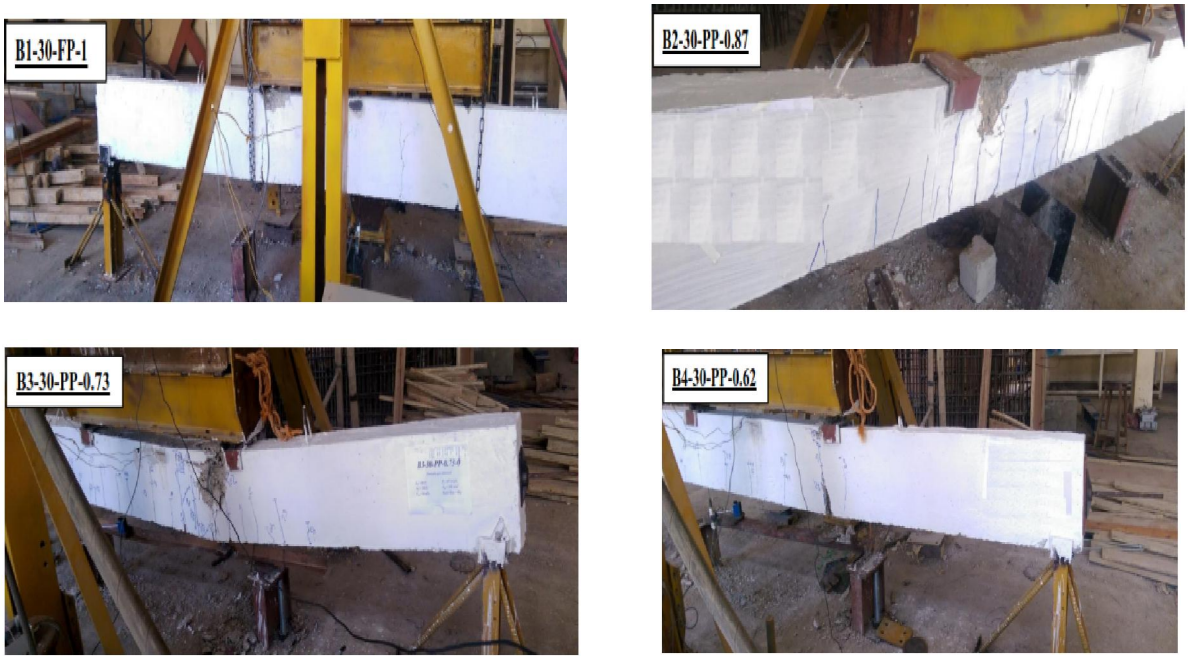

Fig. (6) Crack patterns at failure of all tested beams

Table (3) Summarize the details of the test process of all the tested beams

Parameters	Beam specimens			
	B1-25-FP-1	B2-25-PP-0.87	B3-25-PP-0.73	B4-25-PP-0.62
Cracking load Pcr (kN)	37.08	29.3	26.5	17.2
Yielding load Py (kN)	-----	92.7	72.1	39.94
Max. load Pmax (kN)	107.8	111.83	95.9	64.5
Ultimate load Pu (kN)	86.24	89.46	68.72	51.6
Ult. deflection Δ (mm)	54.12	68.8	61.6	47.96
Failure cycle	70	86	93	74
Failure patterns	Many parallel vertical cracks at pure bending especially at the mid-span of the beams where the moments are large. A few inclined cracks could be observed at flexure-shear sections and Concrete crushed and spalled off at pure bending sections and loading points with cutting of steel bars at tension side and buckling of longitudinal steel bars at compression side.			

3.2. Hysteresis curves.

Hysteresis curves are load versus displacement relationships of structures under cyclic loading, which can provide understanding for analysis of the dynamic elasto-plastic response. Hysteresis (P–Δ) curves of beams are shown in Fig. (8). Here, P is the applied vertical load at loading beam and Δ is the mid-span deflection of each beam. The followings can be observed from these curves:

1. Before the appearance of the first crack for all specimens, the relationships between vertical loads P and mid-span deflections Δ are basically linear. No

obvious degradation in stiffness could be observed, and residual deformation is almost neglegable; all this shows that all members are basically in the elastic range.

2. After cracking of specimens, hysteresis plot become more curved. The slopes of these curves degrade with increasing load and displacement.

3. By comparing with the maximum load reached in the first cycle, there is little strength decay in partially post-tensioned beams in the next cycles under cyclic load.

4. The stiffness of fully post-tensioned beam at earlier period of loading and unloading is higher than that of partially post-tensioned beams at the corresponding stages. However, the stiffnesses of all specimens in the last period of loading are almost the same.

5. Variable pre-compression values for tested beams resulting in deferent number of cycles until failure. The pre-compression value are 3.3, 3, 2.7, and 2 mPa for tested beams (B1-25-FP-1, B2-25-PP-0.87, B3-25-PP-0.73, and B4-25-PP-0.62) respectively. Each beam need deferent number of cycles until failure, 71, 85, 92, and 74 cycles respectively needed for each specimen to reach failure.

6. B2-25-PP-0.87, and B3-25-PP-0.73undergoes more loading cycles in comparison with B1-25-FP-1, which results from the use of ordinary reinforcement steel in flexural which make the beams more ductile. In addition, decreasing pre-compression value leads to evident degradation in the load-carrying capacity.

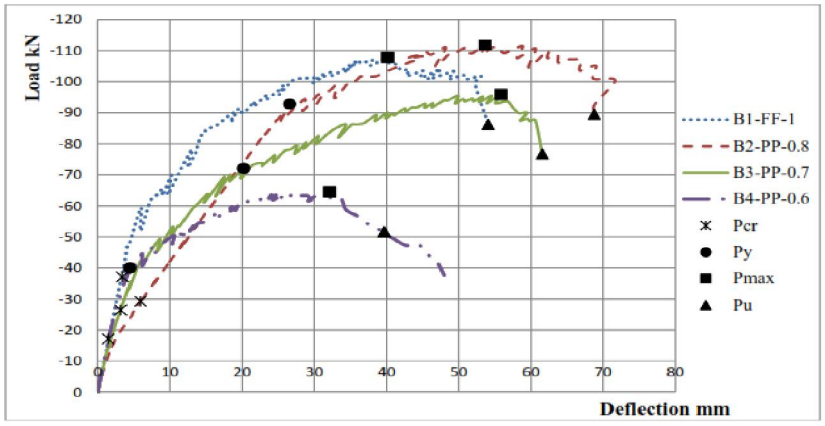

Fig. (7) Total load versus the mid span deflection of all the tested beams.

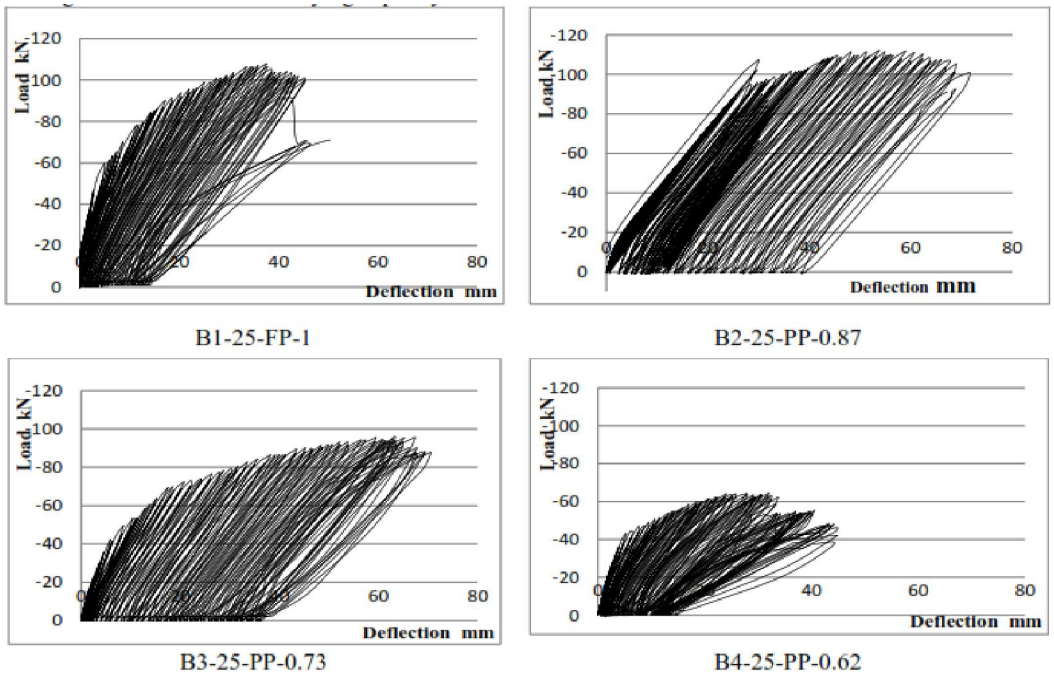

Fig. (8). Hysteresis (P–Δ) curves of beams

3.3. Skeleton curves.

Skeleton curves shown in Fig. (7) are envelopes of hysteresis curves. The followings can be obtained from these figures:

1. Skeleton curves of the four beams could be divided into three phases: the elastic phase, the yield phase, and the ultimate phase.
2. In the elastic phase, the relationships between loads and mid-span deflections in skeleton curves are basically linear before concrete cracking. After the cracking of specimens, the skeleton curves become more curved. When the specimens yield, evident inflexion points could be observed. In the yield phase, slit increase in the vertical loads take place with increasing displacements.
3. No obvious yield points could be observed in the skeleton curves of the fully post-tensioned beams in comparison with the partially post-tensioned beams. This is characteristic of the fully post-tensioned member which is due to the absence of non-post-tensioned steel at tension side.
4. An increase in cracking load in B1-25-FP-1 (fully pre-stressed) is due to high pre-compression value. Also an obvious decrease in ultimate displacement and high load carrying capacity could be observed in the fully post-tensioned beams.
5. An increase in yield loads and yield displacements due to a higher amount of reinforcement could be observed in B2-25-PP-0.87 and B3-25-PP-0.73(partially pre-stressed). Also an obvious decrease in cracking load could be observed in the partially post-tensioned beams.
6. The load carrying capacity of B1-25-FP-1 (fully pre-stressed) and B2-25-PP-0.87 (partially pre-stressed). quite close to each other, indicating that relatively low addition of non-pre-stressed steel has little effect on the load carrying capacity of beams.
7. An obvious decrease in cracking load, yield load, ultimate displacement, and load-carrying capacity in B4-25-PP-0.62 is probably due to very high non-pre-stressed steel and low pre-compression value.
8. The Failure of fully post-tensioned beams occurs earlier than partially post-tensioned beams in cycles. A descending branch could be observed after the yielding of partially post-tensioned beams, indicating that pre-compression value make no apparent contribution to the load-carrying capacity of post-tensioned beams, while however enhancing the displacement ductility of partially post-tensioned beams.

3.4. Deformation restoring capacity.

Structures are always in the elasto-plastic range during strong dynamic loading. The deformation restoring capacity and residual deformation directly affect the rehabilitation and serviceability of structures. In this paper, the residual deformation ratio, which is defined as $\Delta r / \Delta u$ [5], is used as a key index for evaluating the deformation restoring capacity of beam specimens. Here, Δr is the residual displacement after unloading and Δu is equal to the maximum displacement for skeleton curves without the descending part or equal to the displacement corresponding to 85% maximum load in the descending part of the skeleton curves. The parameters for the restoring behavior of beams are presented in Table (4).

Table (4). parameters for the restoring behavior of beams

parameters	Beam specimens			
	B1-25-FP-1	B2-25-PP-0.87	B3-25-PP-0.73	B4-25-PP-0.62
Δr (mm)	6.5	36.24	44.89	16.53
Δu (mm)	58.7	71.42	75.41	47.19
$\Delta r / \Delta u$	0.11	0.51	0.6	0.35

As shown in the table, the following could be obtained:

1. The residual deformation ratios of the fully post-tensioned beam are about 0.11, indicating that beam display relatively small deformation restoring capacities.
2. The residual deformation ratio of partially post-tensioned beams are about 0.35-0.51, indicating that beam display relatively large deformation restoring capacities than that of fully post-tensioned beam. That is due to the use low pre-compression value and higher amount of non-pre-stressed steel.
3. The residual deformation ratio of B3-25-PP-0.73 during loading is a little higher than that of B2-25-PP-0.87at corresponding loading stages. Conclusions can be drawn that using high value of pre-compression makes obvious contribution to the deformation restoring capacity beams.
4. The residual deformation ratio of B2-25-PP-0.87 and B3-25-PP-0.73 is higher than that of B1-25-FP-1, which indicates that an increase in the reinforcement ratio has obvious influence on the deformation restoring capacity of pre-stressed beams.
5. Higher increase in the non-pre-stressed steel with lower pre-compression value would lead to a decrease in the deformation restoring capacity by comparing the residual deformation ratios of B2-25-PP-0.87 and B3-25-PP-0.73. but not a benefit because it obviously affected the overall beam behavior in term of cracking load, load carrying capacity, and ultimate deformation.
6. The residual deformation ratios of fully post-tensioned beams are obviously lower than those of the

partially post-tensioned beams at corresponding loading stages, reflecting that the applying full pre-stressing in beams results in a reduction in residual deformation. This also means that the fully post-tensioned beams behave in a better deformation-restoring manner, thus they are much more convenient for rehabilitation in comparison with partially post-tensioned beams.

3.5. Displacement ductility.

Displacement ductility is used as an important index for the dynamic evaluation of structures. The ductility coefficient μ, representing the ratio of ultimate displacement (Δu) to yield displacement (Δy), is defined as Δu/Δy [5].Δy is equal to the displacement corresponding to the yielding of the beam specimens. The measured ductility coefficients of beams at each characteristic point are presented in Table (5).

Table (5) Measured ductility coefficients of tested beams.

parameters	Beam specimens			
	B1-25-FP-1	B2-25-PP-0.87	B3-25-PP-0.73	B4-25-PP-0.62
Δy (mm)	32.6	26.49	30.4	23.58
Δu (mm)	58.7	71.42	75.41	47.19
μ = Δy / Δu	1.8	2.69	2.48	2

The following conclusions can be drawn:

1. The maximum displacement ductility coefficient (2.69) is achieved in B2-25-PP-0.87, while the minimum displacement ductility coefficient (1.8) occurs in specimen B1-25-FP-1. Conclusions can be drawn that the partially post-tensioned beams behave in a more ductile manner than fully post-tensioned beams.
2. It also can be observed that in partially post-tensioned beams displacement ductility could be increased by using high pre-compression value in B2-25-PP-0.87 by comparing the ductility coefficients of B3-25-PP-0.73 and B4-25-PP-0.62.
3. The displacement ductility coefficient of B2-25-PP-0.87is about 2.69, which is higher than that of B3-25-PP-0.73. This can be attributed to the use of less non-pre-stressed steel.
4. The displacement ductility coefficients of fully post-tensioned beams are apparently lower than those of partially post-tensioned beams, displaying that the applied fully pre-stressing could decrease the ductility of specimens and that of non pre-stressed steel could increase the ductility of specimens.
5. By comparing B1-25-FP-1 with B2-25-PP-0.87, it could be observed that the displacement ductility of the pre-stressed beams could be improved significantly by using ordinary reinforcement.
6. Higher increase in the ordinary reinforcement leads to a decrease in the displacement ductility of the pre-stressed beams as shown from comparing the displacement ductility coefficients of B2-25-PP-0.87and B3-25-PP-0.73.

3.6. Stiffness degradation.

The stiffness, which is defined as K = P/Δ, is used for describing the stiffness degradation of specimens, where P is the applied vertical load at the two loading points and Δ is the mid-span deflection of beams. The stiffnesses of the four beams during testing is shown in Fig. 9. Conclusions can be drawn as follows:

1. The stiffness of all beams evidently degrades from cracking to yielding, but remains almost constant after yielding. However, obvious stiffness degradation still occurs in fully pre-stressed beams after yielding.
2. An increase in the reinforcement ratios would slow down the degradation speed of stiffness in partially post-tensioned beams by contrasting with the other fully post-tensioned beams. It could also be observed that the use of low pre-compression value have obvious relationships to stiffness degradation in beams. It also shows that the stiffness of the fully post-tensioned beams degrades more slowly in earlier period of loading than that of the partially post-tensioned beams.
3. At earlier loading period the stiffnesses at each displacement control point of the post-tensioned beams with low pre-compression value and with higher reinforcements are larger than the beams with high pre-compression value due to larger load-carrying capacities.

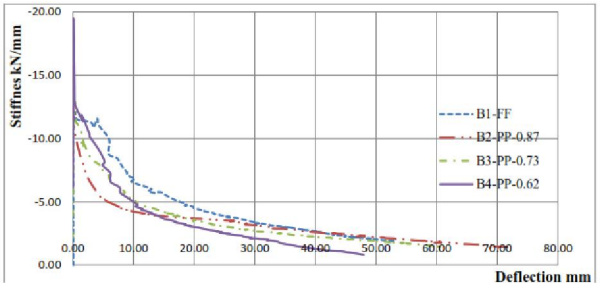

Fig. (9) Stiffness degradation of all tested beams Stiffness degradation of all tested beams

3.7. Energy dissipation capacity.

The energy dissipated during a single load cycle is calculated using the Trapezoid rule to determine the area within the curve of vertical load (P) versus mid-span deflection (Δ). The amount of energy dissipated in the four beams during testing is shown in table. (6). the dissipated energy of the Four beams during testing is shown in Fig. 10. The following could be achieved:

Table (5) Measured energy dissipation capacity of tested beams.

parameters	Beam specimens			
	B1-25-FP-1	B2-25-PP-0.87	B3-25-PP-0.73	B4-25-PP-0.62
Total energy dissipated (kN.mm)	16300	23500	22300	13200
PPR Ratio	1	0.87	0.73	0.62
% of increase	Control	44.1%	36.8%	-20.1%

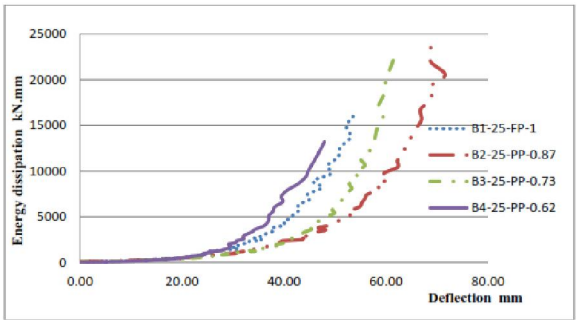

Fig. (10) Measured energy dissipation capacity of tested beams.

1. Very small value of energy has been dissipated in all tested beams before concrete cracking. The amount of energy dissipated in the elasto-plastic phase increases clearly with increasing displacements.

2. No evident relationship between the longitudinal reinforcement ratios and the energy dissipation could be observed before the yielding of specimens.

3. It could also be observed clearly that much more energy has been dissipated in the partially post-tensioned beams than in the fully post-tensioned beams.

4. Tests also show that greater reinforcement results in an increased energy dissipation capacity in post-tensioned beams at the large-displacement stage. The dissipated energy increases highly in partially post-tensioned beams than fully post-tensioned beam in the last period of loading. The use of conventional steel is favorable for the dissipation of energy in post-tensioned beams at the large-displacement stage, which could be observed from specimens B2-25-PP-0.87 and B3-25-PP-0.73.

5. In contrast to B2-25-PP-0.87 and B3-25-PP-0.73, the energy dissipated in B4-25-PP-0.62 increases much more slowly in the last period of loading, reflecting that much increase in conventional steel of B4-25-PP-0.62 is not favorable for energy dissipation in the post-tensioned beams.

6. At the large-displacement stage, the amount of energy dissipated in B4-25-PP-0.62 decreases than that dissipated at fully post-tensioned beam due to the low pre-compression value and high reinforcement ratio.

7. By comparing B2-25-PP-0.87 and B3-25-PP-0.73, the amount of energy dissipated in post-tensioned beams during the last period of loading is about 36.8%–44.1% higher than that of B1-25-FP-1 due to the effect of using conventional steel.

4. Conclusions.

Experimental uni-directional cyclic loading tests of fully and partially post-tensioned beams are conducted in this paper. Based on the results of this study, the following conclusions can be stated:

1. Most of partially post-tensioned beams did not reach their designed ultimate capacity. Such as specimens B3-25-PP-0.73 and B4-25-PP-0.62 their ultimate failure load decreased by 13 kN and 57 kN respectively. The decrease was regarded to the effect of cyclic loading.

2. The cracking load of fully post-tensioned beam is much higher than that of partially post-tensioned beams. Fully post-tensioned beam cracked at 37 kN, while the partially post-tensioned beams cracking load ranged from 17.2 to 29.3 kN. This can be regarded to the high pre-compression value at fully post-tensioned beam.

3. An obvious increase in maximum deflection of partially post-tensioned beams than that of fully post-tensioned beam. The maximum deflection of partially post-tensioned beams ranged from 47.96 mm to 69 mm, while deflection of fully post-tensioned beam was 54.14mm.

4. Partially post-tensioned beams dissipated large amount of energy than fully post-tensioned beam. The energy dissipation capacity of partially post-tensioned beams ranged from 13200 to 23500 kN.m, while energy dissipation capacity of fully post-tensioned beam was 16300 kN.m.

5. Residual deformation in partially post-tensioned beams was much higher than that of fully post-tensioned beams. The residual deformation ratios of partially post-tensioned beams range from 0.35 to 0.51. The residual deformation ratios of the fully post-tensioned beams (about 0.11, indicating that the fully post-tensioned members behave with relatively high deformation restoring capacity.

6. Partially post-tensioned beams exhibited an increase in displacement ductility coefficient ranged from 12% to 49.5% higher than fully post-tensioned beam, indicating that partially post-tensioned beams behave more ductile than fully post-tensioned beams.

7. The stiffness degradation of partially post-tensioned beams mainly was much higher than that of fully post-tensioned beams. Indicated that increasing P/A ratio decrease the stiffness degradation.

Reference

1. ACI Committee 318. Building Code Requirements for Structural Concrete (ACI 318–2014) and Commentary (ACI 318–2014). American Concrete Institute, 2014.
2. A. E. Naaman, Presressed Concrete Analysis and Design, McGraw Hill, NY, 1982, p. 670.
3. H. Manalip, M. Pinglot, M. Lorrain, Behavior of the compressed zone of reinforced and prestressed high strength concrete beams, ACI Journal 149 (1994) 209–226 (SP149-12).
4. Xiao Yan, Ma Rui. Seismic behavior of high strength concrete beams. The Structural Design of Tall Buildings 1998;7:73–90.
5. Weichen Xue, Liang Li, Bin Cheng, Jie Li. The reversed cyclic load tests of normal and pre-stressed concrete beam. Engineering Structures 30 (2008) 1014–1023.

3/13/2018